




Performance of soft/hard composite dual-effect coated tool in dry cutting of carbon fiber–reinforced polymer

Tianyuan Zhang¹ · Yangyang Long² · Chenliang Mu³ · Wei Zhou¹ · Guolong Zhao⁴ · Yunsong Lian^{1,4} 

Received: 25 February 2020 / Accepted: 13 July 2020 / Published online: 28 July 2020
© Springer-Verlag London Ltd., part of Springer Nature 2020

Abstract

Carbon fiber–reinforced polymer (CFRP) is a difficult-to-machine material whose machining requires cutting tools of high performance. In this study, a CrCN-WS₂ dual utility coated tool (the tool is a composite of the hard coating CrCN and the soft coating WS₂) was used to improve the dry cutting performance of CFRP. To validate the improvement of the CrCN-WS₂ dual utility coated tool, three other different tools including uncoated tool, CrCN hard-coated tool, and WS₂ soft-coated tool were applied to do the dry cutting test. The three-axis cutting force, the cutting temperature, the average friction coefficient, the three-dimensional shape of the rake face, and the height of the cohesive section were measured. The results revealed that the CrCN-WS₂ dual utility coated tool has the best cutting performance and is more suitable for turning CFRP materials among the four tools. Since it can fully combine the high hardness and high wear resistance of CrCN and the friction reduction of WS₂, the cutting force and the cutting heat were effectively reduced, and the rake face condition was greatly improved.

Keywords CrCN-WS₂ dual utility coated tool · Cutting performance · Dry cutting · CFRP

1 Introduction

Carbon fiber–reinforced polymer (CFRP) has a high specific strength, a high specific modulus, a high damping capacity, a good dimensional stability, excellent resistance to deformation, and good corrosion resistance and fatigue resistance [1–3]. Therefore, it is widely used in aerospace, robotics, medical, and military industries. [4–7]. However, CFRP material is discontinuous in the cutting process due to its forming structure (microfiber braided lamination plus epoxy resin bonding),

which leads the cutting tool suffering a relatively large discontinuous impact force, so the cutting force of the tool was fluctuated in a large range. This will bring a series of problems to the processing of CFRP, such as poor quality of machined surface and damage of tool. Hence, high-performance cutting tools are demanded to the machining of this difficult-to-machine material. Wang et al. [8] stated that the most common tools for cutting CFRP are diamond tools, diamond-coated tools, and some wear-resistant coated tools (such as AlTiN coating) at present. In addition, due to the unique molding method and the difficult-to-machine characteristic of CFRP material, the cutting environment of CFRP is extremely harsh, which can cause serious tool wear, such as bond wear and abrasive wear [9]. Many scholars researched the effect in increasing tool life of diamond tools, AlTiN-coated tools, and diamond-coated tools recently; they have usually found that the diamond-coated tools have the longest lifespan [10–12]. The cost, however, is high, and the diamond material is brittle, which easily leads to the fracture failure, according to Kwon et al. [13] and Karpat et al. [14]. Other wear-resistant coated tools have a shorter service life and cannot meet the requirements of normal CFRP cutting applications [15]. Therefore, it is necessary to study a novel, durable, and low-cost coated tool for turning in order to process CFRP with high quality.

✉ Guolong Zhao
zhaogl@nuaa.edu.cn

✉ Yunsong Lian
liansy@xmu.edu.cn

¹ Department of Mechanical and Electrical Engineering, Xiamen University, Xiamen 361102, People's Republic of China

² Institute of Dynamics and Vibration Research, Leibniz Universität Hannover, Appelstr. 11, 30167 Hannover, Germany

³ Shanghai Aerospace Control Technology Institute, 1555 Zhongchun Road, Shanghai 201109, People's Republic of China

⁴ Jiangsu Key Laboratory of Precision and Micro-Manufacturing Technology, Nanjing University of Aeronautics and Astronautics, Nanjing 210016, People's Republic of China

Table 1 Mechanical properties of carbon fiber–reinforced polymer (CFRP)

National standard	Tensile strength (MPa)	Tensile modulus (GPa)	Linear density (g/1000 m)	Volume density (g/cm ³)	Elongation (%)	Diameter (μm)	Carbon content (%)
GQ3522	3530	230	198	1.76	1.5	7	93

The research on the milling and drilling of CFRP has been very extensive, while little research has been conducted on the turning of CFRP [16, 17]. Kwon et al. [13] studied the wear of coated drill bits during CFRP drilling. It was found that the ultra-hard diamond-coated drill bit significantly reduced the edge wear of the drill bit which was the main form of wear for all types of drill bits during CFRP drilling; the AlTiN-coated drill bit could not effectively decrease the wear of the drill bit due to its susceptibility to oxidation during drilling. Gaugel et al. [18] found that the wear form of the uncoated cemented carbide drill bit when drilling CFRP was mainly abrasive wear while the diamond-coated drill bit wear was mainly due to partial coating fragmentation. The service life of diamond-coated drill bits was increased by at least 8 times compared with that of uncoated carbide drills. This shows that coated tools can reduce tool wear, improve cutting performance, and extend its service life effectively. However, there are few studies on cutting tools suitable for turning CFRP.

A large amount of cutting fluid which is usually consumed in the processing of difficult-to-machine materials can bring many problems [19]. Abdalla et al. [20] reported that at least two-thirds of the hundreds of thousands of tons of cutting fluid annually consumed by EU countries are not properly disposed. Lian et al. [21] has shown that cutting fluid cost accounts for 15–17% of the total cost of production. But the tool cost only account for 2–4% of it [22]. Lawal et al. [23] stated that the traditional cutting fluid contains many kinds of refractory and toxic substances, which are harmful to the environment and human bodies. For the purpose of reducing the harmfulness brought by cutting fluids, dry cutting tests of CFRP were carried out in this study, which can not only reduce the manufacturing costs but also protect the environment and human health. Green manufacturing is a hotspot in the international society [24]. Dry cutting technology is a new type of cutting technology aiming at the pollution of cutting

fluid and high cost [25, 26]. The cutting fluids have the function of lubrication and cooling, which is beneficial to reduce the cutting temperature, extend the lifespan of tool, and improve the machining accuracy. Because the tool wear is severe without cutting fluid, a novel coating tool for CFRP dry cutting is proposed to improve the wear resistance.

In the view of the above problems, a CrCN-WS₂ dual utility coated tool that meets green cutting requirements and has excellent performance was proposed to cut CFRP. This coating consisting of a hard layer of CrCN and a soft layer of WS₂ was supposed to combine the high hardness and wear resistance of CrCN and the antifriction performance of WS₂. This study used the dual utility coated tool to cut CFRP material without cutting fluid, and the uncoated tool, the hard coated tool of CrCN, and the soft coated tool of WS₂ were added to it for comparison. The three-axis cutting force and the cutting temperature were measured through the turning test, then the average friction coefficient on the rake face is analyzed, and the wear of the rake face and chip was measured by SEM and LSCM form. The cutting performance of CFRP of the CrCN-WS₂ dual utility coated tool was obtained through comparative and comprehensive analysis of these indicators.

2 Experiments

2.1 Preparation of cutting tool and workpiece

The CFRP bar with an outer diameter of 55 mm and an inner diameter of 20 mm was customized by Weihai Guangwei Composite Materials Co., Ltd. The T300 grade fiber according to the China national standard GQ3522 was selected and was unidirectionally woven into preregs (its mechanical properties are shown in Table 1) with angles of 0°, 90°, and ±45°. Then the preregs with different weaving angles were mixed with the 6511 type resin to prepare the bar with a resin ratio of 30% in volume.

Table 2 Physical properties of the YS8 ultra-fine-grained cemented carbide blade

Cutting tool	Hardness (HRA)	Flexural strength (MPa)	Density (g/cm ³)	Young's modulus (GPa)	Thermal expansion coefficient (× 10 ⁻⁶ °C ⁻¹)	Poisson's ratio
YS8	92.5	1720	13.9	550	5.5	0.27

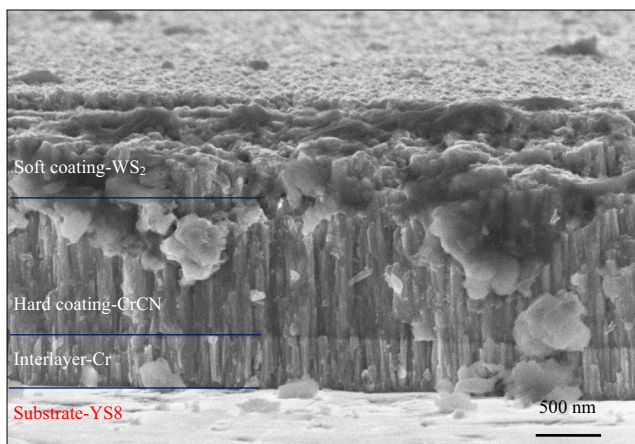
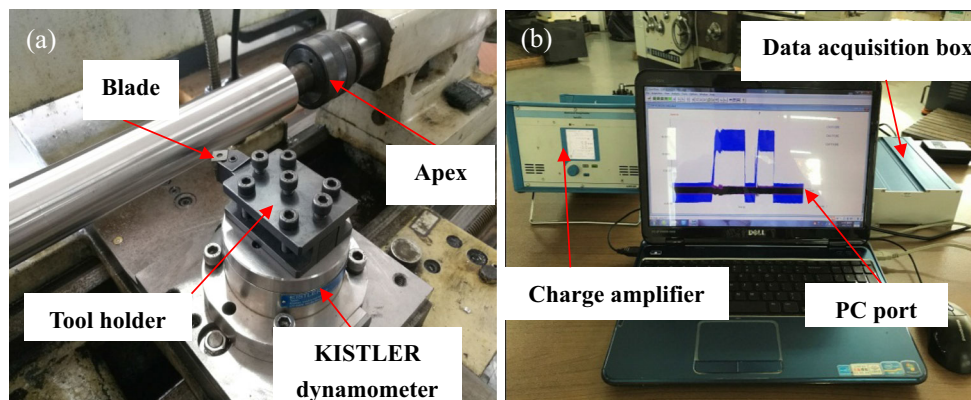


Fig. 1 Section morphology of CrCN-WS₂ dual utility coating

The tool base in this work was the ultra-fine grain carbide indexable insert (YS8-41305N) produced by Zhuzhou Cemented Carbide Cutting Tools Co., Ltd. Ninety-five percent of the blade material is WC; the balance is the binder Co and a small amount of TiC [27]. Compared with conventional carbide inserts, the ultra-fine-grained carbide reduces the amount of the binder Co and improves the hardness and wear resistance of the insert. The physical properties of the blade are given in Table 2. The blade was prepared in the geometry of 12.5 mm × 12.5 mm × 4.5 mm with a tip radius of 0.5 mm.

As shown in Fig. 1, the prepared CrCN-WS₂ dual utility coating includes three layers: the transition layer Cr-0.4 μm, the hard coating layer CrCN-1.8 μm, and the soft coating layer WS₂-0.8 μm. The transition layer Cr was prepared by the method of DC magnetron sputtering in argon, and the target is pure Cr. The hard coating CrCN was made by RF-reactive magnetron sputtering in nitrogen and argon, the target is Cr₃C₂. And the soft coating was deposited by electrospinning. The physical and mechanical properties of the obtained CrCN-WS₂ dual utility coating were as follows: the bonding force between this coating and the tool is 52 N, and the hardness of CrCN is 2700 HV.

Fig. 2 Turning test site layout: (a) lathing and (b) data processing



All the turning tests were conducted on a CA6136 lathe. In order to reflect the superior performance of the CrCN-WS₂ dual utility coating tool, all turning tests are dry cutting without cutting fluid.

2.2 Selection of cutting parameters

As shown in Fig. 2, the indexable insert and the tool holder integrated with the dynamometer were mounted on the CA6136 engine lathe. The signal from the dynamometer was transmitted to the charge amplifier and then collected by the PC through the data acquisition box.

In the turning test, the recommended cutting parameters of other difficult-to-cut materials were referred, and the three elements of this turning test were designed and tested. Based on the findings of this trial, when the cutting depth was greater than 0.7 mm, the deep carbon fiber layer of CFRP has been cut, but the surface and shallow carbon fiber layer were still attached to the workpiece and rotated together with the bar at a high speed. This high-speed rotation of the uncut fiber layer created a successive impact on the rake face of the tool, which greatly reduced the tool life and the cutting effectiveness. In addition, the tool significantly vibrated when the cutting speed and the feed rate were high. The high temperature generated would lead to the degradation of the resin with a low thermal conductivity [28]. In summary, the cutting depth of the CFRP bar should not exceed 0.7 mm to reduce the above-mentioned adverse effects, and the cutting speed and feed rate should not be too large. Therefore, the three parameters of cutting CFRP in this work were as follows: cutting depth $a_p = 0.5$ mm, feed rate $f = 0.2$ mm/r, and cutting speed $v = 80\sim 200$ m/min.

2.3 Cutting tests and measurements

In this work, to analyze the cutting performance of CrCN-WS₂ dual utility coated tool, three other tools were tested as a contrast. The uncoated tool is named as NT, the tool with the hard coating CrCN is named as CT, the tool with the soft coating WS₂ is named as WT, and the CrCN-WS₂ dual utility

Table 3 Cutting parameters employed for dry turning tests with CFRP

Test	Tool type	Cutting speed v (m/min)	Feed rate f (mm/r)	Cutting depth a_p (mm)	Rake angle γ_0 (°)	Relief angle α_0 (°)	Cutting edge angle K_r (°)	Edge inclination angle λ_s (°)
1	NT, CT, WT, CWT	80	0.2	0.5	−5	5	45	0
2		110						
3		140						
4		170						
5		200						

coated tool is named CWT; the base of all tools is YS8 ultra-fine-grained carbide. Cutting parameters for the dry turning tests with CFRP are shown in Table 3.

The cutting force and the cutting temperature were collected during the cutting process. The blade and the chips after cutting were observed and analyzed. During the test, the three-axis cutting force was real-time measured by the dynamic force measurement system (KISTLER9272, Swiss). The portable high-performance infrared thermal imager (C640, Guide Inc., China) was used to capture the cutting temperature within the cutting area. The measurement range of the thermal imager is $-20\sim 800$ °C. After the cutting test, a laser scanning confocal microscope (LSCM) (KEYENCE VK-X250) and a field emission scanning electron microscope (SEM) (ZEISS SUPRA 55) were used to analyze the wear and the adhesion of the blade.

Figure 3 illustrates the cross-section of CFRP and the machined surface after turning. The lamination structure of the CFRP bar can be clearly observed. And the mechanical properties and roughness of the resin layer and the carbon fiber layer are different. Owing to the non-uniformity and anisotropy of the CFRP, the processing of the CFRP material can cause the pulling out of fibers and the debonding of the fiber matrix, which brings many uncertain factors to the machined surface roughness [29]. Therefore, the roughness of the machined surface is not used as an indicator to judge processing performance of tool in the CFRP turning test.

It is worth noting that since the raw material of the CFRP bar was made of fiber with a diameter of $7\ \mu\text{m}$, the chips are produced in powder form during the turning process as shown in Fig. 4. In addition, some uncut fibers on the surface layer rotate at high speed to drive air flow, which causes dust pollution during the cutting process and may cause fire. Therefore, the tester must wear a mask and prepare a carbon dioxide fire extinguisher.

3 Results and discussions

3.1 Cutting forces

Figure 5 shows the three-axis cutting forces of the four cutting tools during CFRP cutting under the conditions of $v = 200$ m/min, $f = 0.2$ mm/r, and $a_p = 0.5$ mm. It can be seen from the figure that the three-axis cutting forces of CWT are the lowest. But the three-axis cutting force is less reduced than the traditional uncoated tool NT, and the main cutting force F_z , the radial thrust F_y , and the feed force F_x are reduced by 10.2%, 12.6%, and 17.5%, respectively. In addition, the cutting forces of the four tools cutting CFRP are small, but the cutting force has a large oscillation range that is ± 15 N of the average cutting force during the cutting process. The main reason for this phenomenon is that CFRP whose structure is laminated fiber belongs to difficult-to-cut materials. So the process of

Fig. 3 The images of cross-sectional morphology of CFRP and surface morphology after turning

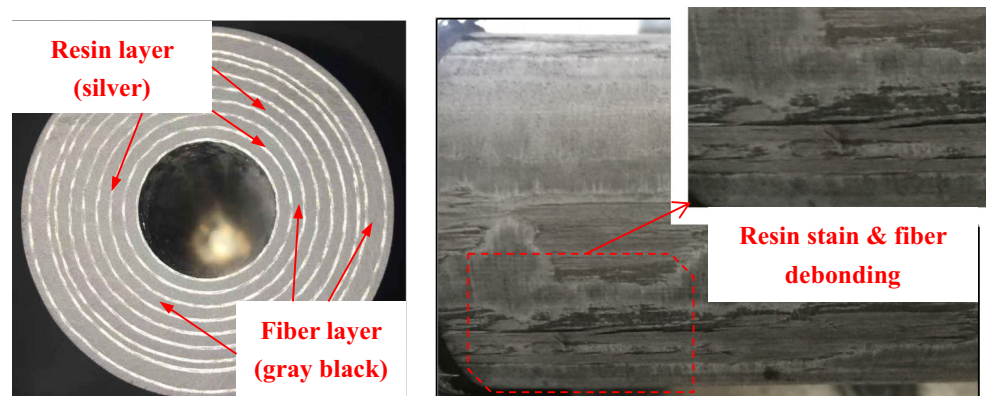




Fig. 4 Powdered chips during the turning of CFRP bars

turning CFRP is continuously accompanied by the fiber breakage and the cutting of the new fiber layer, and the cutting force is in a period of constant oscillation that causes considerable impact for the tool. In other words, in order to improve the performance of turning CFRP material, it is necessary to make the impact resistance of the tool be fine.

The CrCN-WS₂ dual utility coated tool has limited effect on improving the performance of cutting CFRP. This was because that soft coating WS₂ was quickly shattered due to the strong impact produced by the fiber cutting and the high-speed rotation impact of uncut fiber on the tool rake face; the hard coating CrCN was then exposed. The coating withstood

the changing forces owing to the intense impacts, which makes the coating to be easily damaged by shattering [10, 30].

Figure 6 illustrates the changes of the three-axis cutting force of the four tools at five different cutting speeds (80~200 m/min), with the cutting depth of 0.5 mm and the feed rate of 0.2 mm/r. In general, the differences of the cutting forces among different tools are not large, but it is obvious that the CrCN-WS₂ dual utility coating tool (CWT) has the smallest cutting force among the four tools. Compared with the NT, the main cutting force F_Z of CWT decreased by 2.4~12.1%, the radial thrust F_Y decreased by 12.4~40.2%, and the feed force F_X decreased by 15.0~32.1%. Especially when the cutting speed was 170 m/min, the three-axis cutting forces were both decreased. The reduction of its cutting force decreased the normal force and friction force on the rake face, which can reduce the wear of the tool and improve the quality of processed surface. It indicates that the CrCN-WS₂ dual utility coating tool has a positive effect on improving the cutting performance of CFRP materials, especially at high cutting speeds. In addition, contrast with the main cutting force F_Z of WT, it can be seen that soft coating of WT has almost no promoted effect on cutting CFRP. This is because of the severe vibration during the cutting process and the impact of the uncut fiber, which made the soft coating shatter and get detached quickly. Once the WS₂ soft coating is combined with the CrCN hard coating, the cutting performance was enhanced.

Fig. 5 Three-axis cutting forces of four tools ($v=200$ m/min, $f=0.2$ mm/r, $a_p=0.5$ mm): (a) main cutting force F_Z , (b) radial thrust F_Y , and (c) feed force F_X

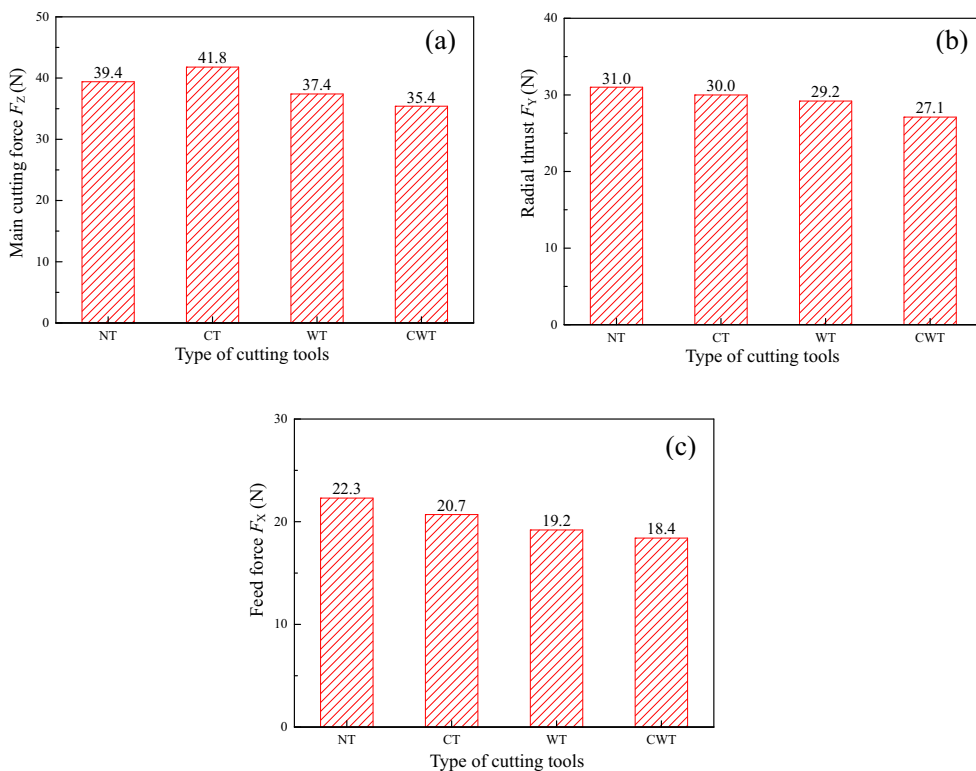
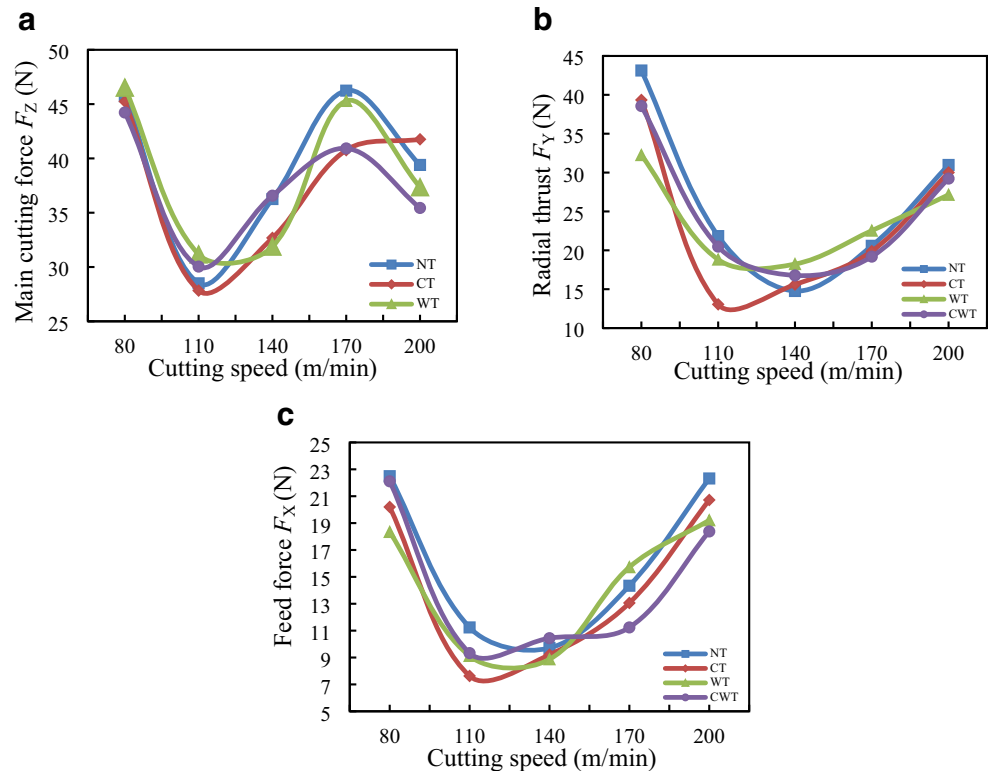


Fig. 6 The three-axis cutting forces of four kinds of tool at five different cutting speeds: (a) main cutting force F_z , (b) radial thrust F_y , (c) feed force F_x



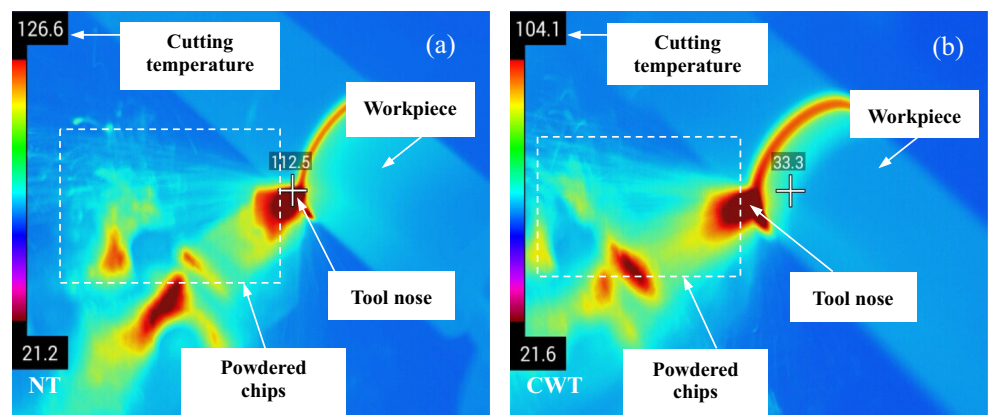
3.2 Cutting temperature

The infrared thermal images of CFRP turned by NT and CWT under the conditions of $v = 140$ m/min, $f = 0.2$ mm/r, and $a_p = 0.5$ mm are shown in Fig. 7a, b, respectively. The highest cutting temperature of NT is 126.6 °C while that of CWT is 104.1 °C. In contrast to conventional NT, the cutting temperature of the CWT decreased by 17.8% under this cutting condition.

Figure 8 shows the changes of the cutting temperature for the four different tools at five cutting speeds. In general, the cutting temperature first decreased and then increased as the cutting speed increased. When the cutting speed was 140 m/min, the cutting temperature was the lowest. The cutting temperature of CWT was the lowest

at any cutting speed. Compared with NT, when the cutting speed was 80 m/min, 110 m/min, 140 m/min, 170 m/min, and 200 m/min, the cutting temperature of CWT was decreased by 31.5%, 18.9%, 17.8%, 17.8%, and 8.0% respectively. It can be seen that as the cutting speed increased, the effect of anti-friction and temperature reduction of the CWT gradually decreased. This is because the shock applied to the coating was greatly enlarged with increasing of the cutting speed. It makes the effect of coating on the cutting performance of CFRP become less obvious, which illustrates that CFRP is a difficult-to-cut material from another point of view. And the cutting temperature of the WT was almost the same as the NT. This is because the bonding force

Fig. 7 The infrared thermal images of CFRP turned by (a) conventional uncoated tool NT and (b) CrCN-WS₂ dual utility coating tool CWT ($v = 140$ m/min, $f = 0.2$ mm/r, $a_p = 0.5$ mm)



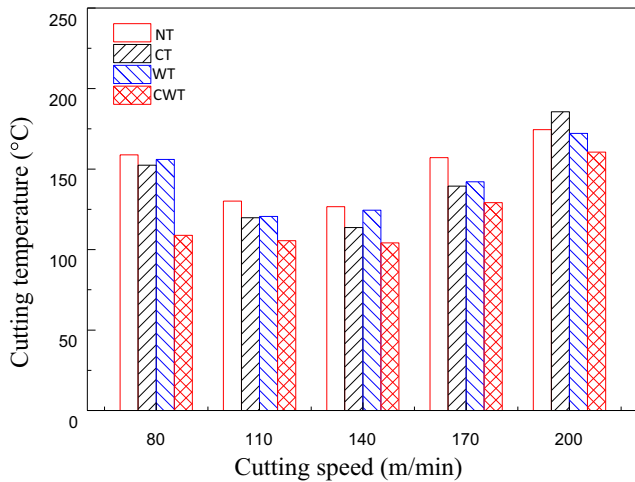


Fig. 8 Cutting temperature of four kinds of tool at five different cutting speeds ($f = 0.2 \text{ mm/r}$, $a_p = 0.5 \text{ mm}$)

between WS_2 and the substrate was poor, and the coating was quickly shattered and detached under the severe vibration shock generated by turning CFRP. The CT has a smaller reduction in cutting temperature than the NT, and its cutting performance is inferior to that of the CWT, which proves again that the effect of compounding the hard and soft coatings is a superposition of the respective effects of the hard and soft coatings.

3.3 Average friction coefficient

Figure 9 shows the average friction coefficients of turning CFRP by four kinds of tools under five cutting speed conditions. As shown in Fig. 9, when the cutting speed was $\geq 140 \text{ m/min}$, the average friction coefficients of

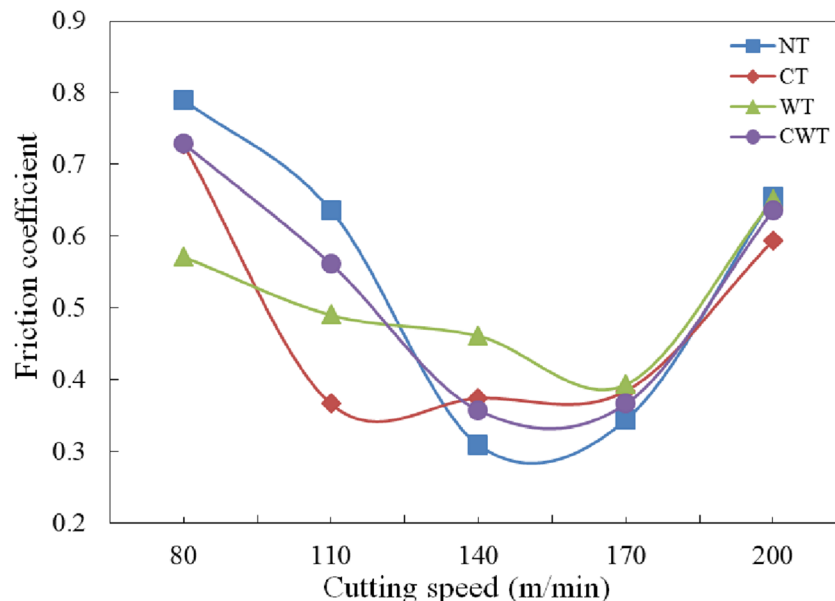


Fig. 9 Average friction coefficient of turning CFRP of four kinds of tools at five different cutting speeds ($f = 0.2 \text{ mm/r}$, $a_p = 0.5 \text{ mm}$)

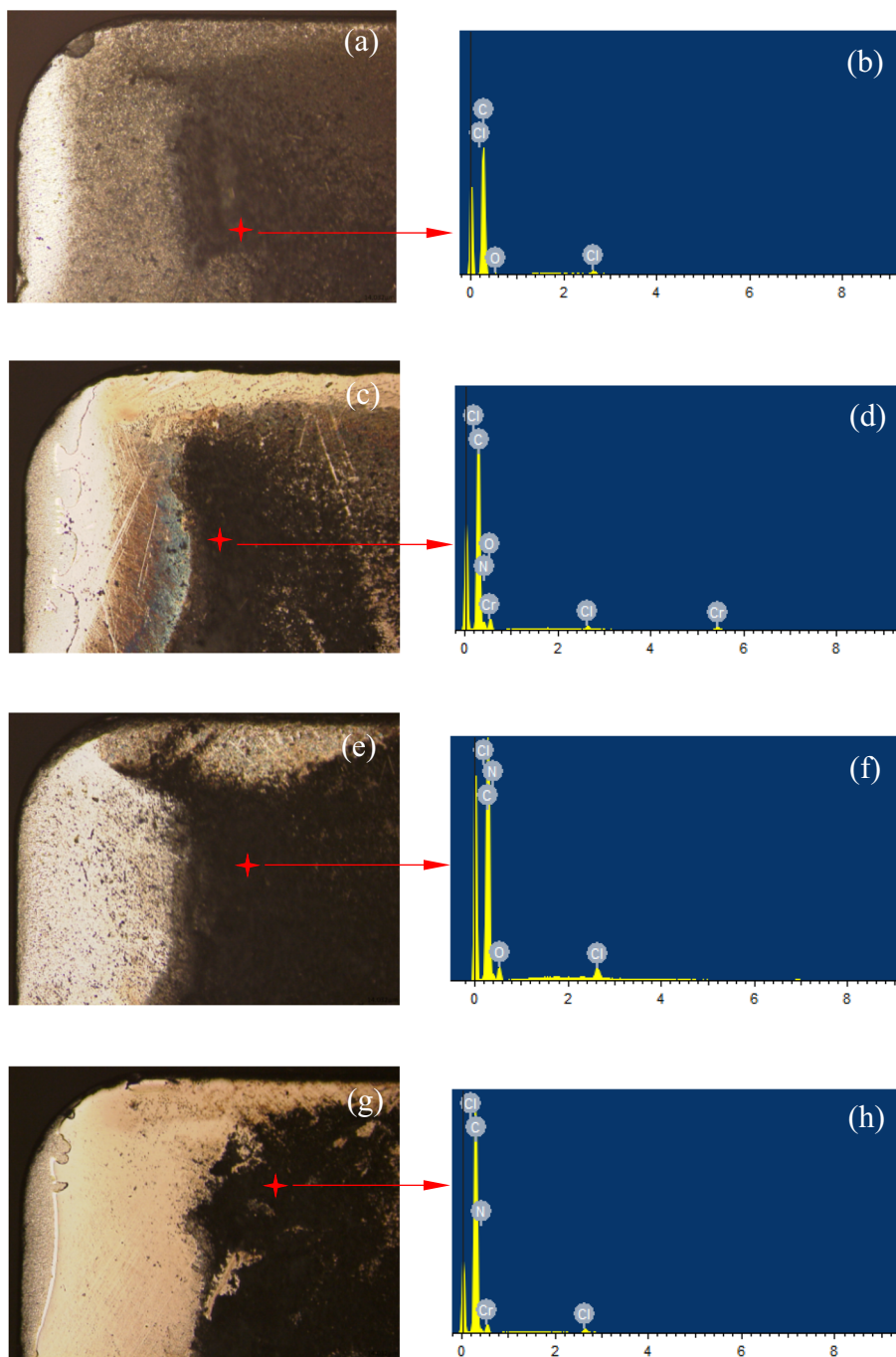
four tools in the turning process had little difference. Thus, the coatings did not show a significant characteristic of friction coefficient reduction. This is probably because when the cutting speed was high, the severe vibration generated during the CFRP turning process made the anti-friction effect of coating less significant. When the cutting speed was 110 m/min , the friction coefficients from low to high were CT, WT, CWT, and NT, and when the cutting speed was 80 m/min , the friction coefficients from low to high were WT, CT, CWT and NT. Therefore, the CrCN- WS_2 dual utility coating tool has a lower friction coefficient characteristic than the soft and hard coatings alone.

3.4 Chip adhesion and wear

Since the carbon fiber is almost black, it is not conducive to the observation in SEM. Hence, the rake faces of the four tools were observed by laser scanning confocal microscopy (LSCM), and components of the adhesive layer were analyzed with energy disperse spectroscopy (EDS). Figure 10 illustrates the two-dimensional shape of rake faces and the EDS analysis of the components of the adhesive layer of four tools when cutting CFRP, and the cutting parameters are $v = 140 \text{ m/min}$, $f = 0.2 \text{ mm/r}$, and $a_p = 0.5 \text{ mm}$.

In general, the bonding area where chips flow of the tool after cutting CFRP is slightly to the lower right of the cutting edge. As shown in Fig. 10b, the EDS detected that the rake faces of four tools were bonded by carbon fiber material. Figure 10a–g show clear peeling off of coating near the cutting edge of the CT and the CWT rake faces. Among them, the falling area of the CT cutter was large and irregular, and the coating breakage

Fig. 10 Bonding morphology and composition analysis of rake faces of four kinds of tools after cutting CFRP ($v = 140$ m/min, $f = 0.2$ mm/r, $a_p = 0.5$ mm): (a) NT rake face, (b) NT bonding composition analysis, (c) CT rake face, (d) CT bonding composition analysis, (e) WT rake face, (f) WT bonding composition analysis, (g) CWT rake face, and (h) CWT bonding composition analysis



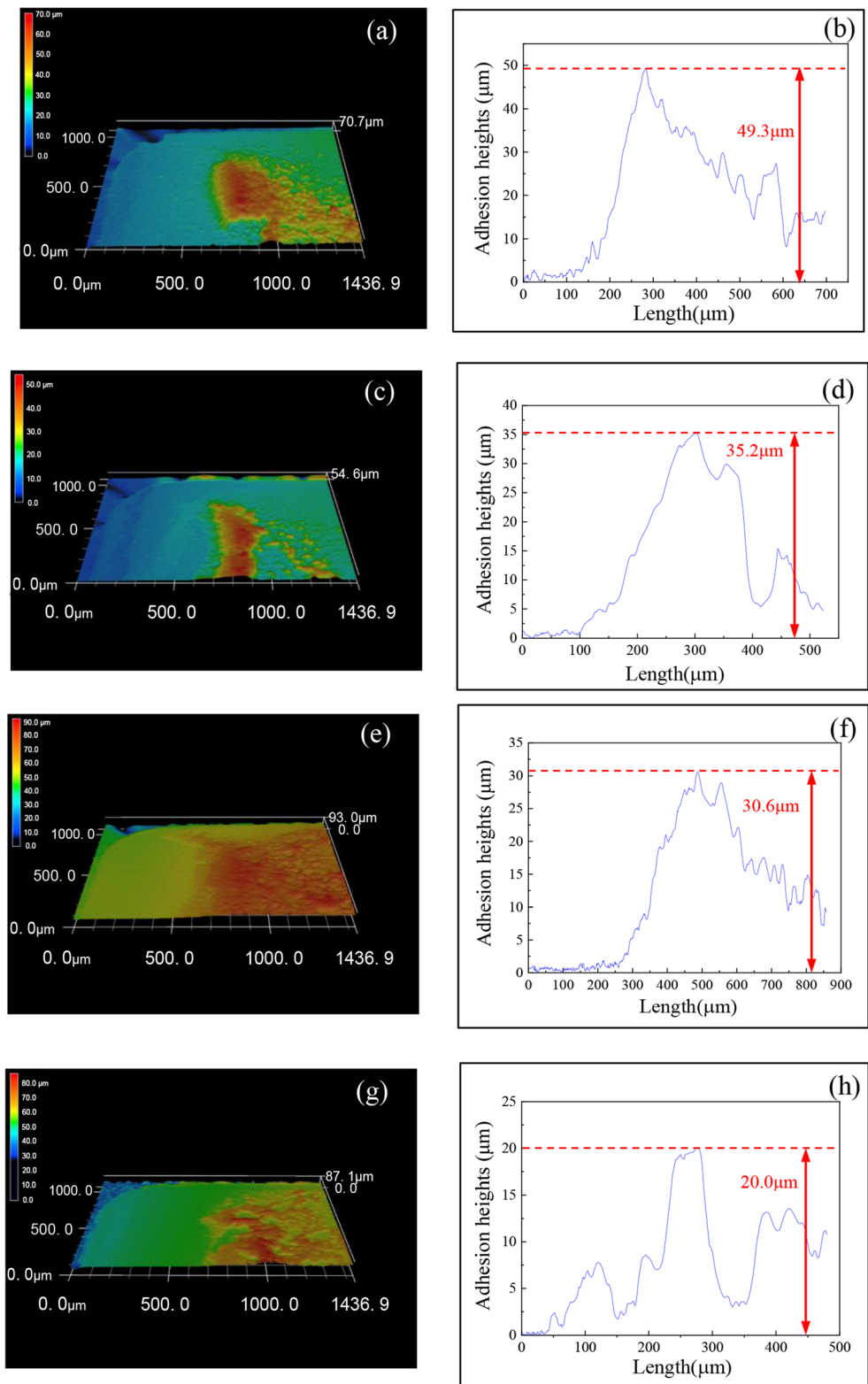
exists, while the coating peeling area of the CWT was the contact area of the chip, which was normal wear. It means that the WS_2 soft coating combined with the hard coating can effectively protect the hard coating and extend the coating life.

Figure 11 shows that the three-dimensional shape of the rake face and the height analysis of the adhesion section after turning CFRP by LSCM under the cutting conditions of $v = 140$ m/min, $f = 0.2$ mm/r, and $a_p = 0.5$ mm. CT, WT, and CWT have different degrees of

reduction in the amount of adhesion compared with NT, which were reduced by 28.6%, 37.9%, and 59.4%, respectively. Therefore, the CWT has a superior anti-adhesive property than the WT and the CT.

Figure 12 shows the average adhesion heights of four tools under different cutting speeds. The adhesion amount of CFRP changed irregularly with the change of the cutting speed. When the cutting speed was 170 m/min, the anti-adhesive properties of CT, WT, and CWT were completely invalid, and the adhesion amount is at a high level. When the cutting speed were 80 m/min,

Fig. 11 Adhesion three-dimensional morphology and cross-sections of rake faces of four kinds of tools ($v = 140$ m/min, $f = 0.2$ mm/r, $a_p = 0.5$ mm): (a) NT three-dimensional bonding morphology, (b) NT adhesion cross-section, (c) CT three-dimensional bonding morphology, (d) CT adhesion cross-section, (e) WT three-dimensional bonding morphology, (f) WT adhesion cross-section, (g) CWT three-dimensional bonding morphology, and (h) CWT adhesion cross-section



110 m/min, 140 m/min, and 200 m/min, compared with NT, the adhesion height of CT was reduced by 39.6%, 34.8%, 28.6%, and 15.6%, respectively; the adhesion height of WT was decreased by 3.6%, 41.2%, 37.9%, and 8.6%, respectively; and the adhesion height of CWT was decreased by 57.8%, 46.0%, 59.4%, and

45.3%, respectively. So, the anti-adhesive property of CWT was better than WT and CT. This is because the CWT combined the super-hard performance of CrCN with the lubricating property of WS₂. The WS₂ soft coating can reduce the friction coefficient of the tool-chip contact surface and improve the processing

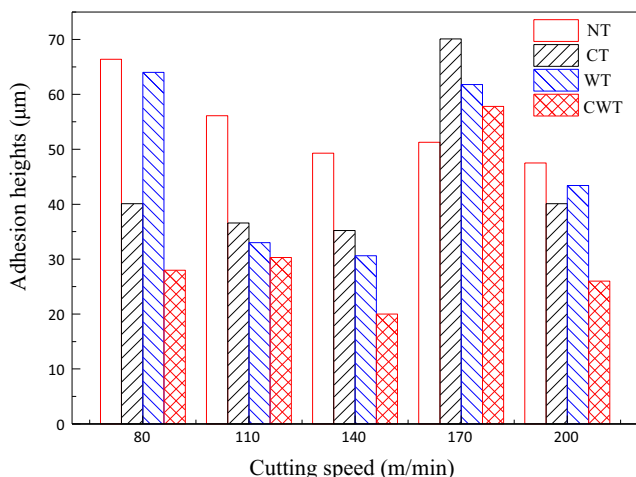


Fig. 12 The adhesion heights of four cutting tools at different cutting speeds ($f=0.2$ mm/r, $a_p=0.5$ mm)

environment of CrCN coating, which made CrCN more wear-resistant and more stable during cutting. Meanwhile, the C element in the CrCN could also reduce the friction coefficient during the cutting process and prolong the service life of the tool.

3.5 Shape of chip

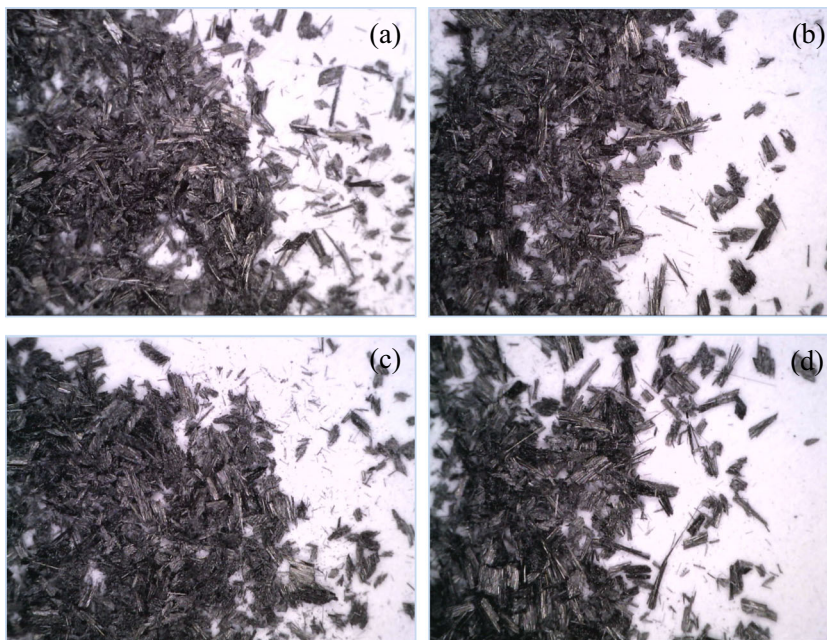
The chip shape changed with the increase of cutting depth. Figure 13 a illustrates the powder shape of the chips when the cutting depth $a_p \leq 0.5$ mm. Figure 13 b illustrates that the chips are a mixture of powder and fiber when the cutting depth 0.5 mm $\leq a_p \leq 0.8$ mm. Figure 13 c illustrates that the chip shape is in the form of fiber floc when the cutting depth $a_p \geq 0.8$ mm.

Due to the special structure of CFRP material and the small amount of the cutting depth ($a_p \leq 0.5$ mm) in the CFRP turn-



Fig. 13 The chip type of CFRP: (a) powdered chips, (b) mixed chips, and (c) floc-shaped chips

Fig. 14 The chip appearances of CFRP after cutting by four cutting tools ($v=170$ m/min, $f=0.2$ mm/r, $a_p=0.5$ mm): (a) chips of cutting CFRP by NT, (b) chips of cutting CFRP by CT, (c) chips of cutting CFRP by WT, and (d) chips of cutting CFRP by CWT



ing experiments in this work, the obtained chips, which macroscopically exist in powder form, have almost no difference as shown in Fig. 13a at any speed with any tool. Figure 14 shows the magnified chip of CFRP cutting by four different tools. There is no difference between the chips during CFRP cutting.

4 Conclusions

In this work, in order to verify the superiority of turning carbon fiber-reinforced polymer (CFRP) with the CrCN-WS₂ dual utility coated tool, the NT, the CT, the WT, and the CWT were applied to turn CFRP under five different cutting speeds. The conclusions are as follows:

- (1) The CWT has the lowest cutting forces among the four tools. Compared with the NT, the main cutting force F_Z was reduced by 2.4–12.1%, the radial thrust F_Y was reduced by 12.4–40.2%, and the feed force F_X was reduced by 15.0–32.1%. Especially when the cutting speed was 170 m/min, the three cutting forces decreased significantly. This proves that the CWT has a positive effect on improving the cutting performance of CFRP materials, especially at high cutting speeds.
- (2) With the increase of cutting speed, the temperature of turning CFRP decreased first and then rose. No matter what cutting speed is used, the temperature of CWT is the lowest. When the cutting speed was 80 m/min, 110 m/min, 140 m/min, 170 m/min, and 200 m/min, in contrast with the NT, the cutting temperature of CWT decreased by 31.5%, 18.9%, 17.8%, 17.8%, and 8.0%, respectively.
- (3) When the cutting speed $v \geq 140$ m/min, the average friction coefficients of the four tools on rake face have little difference. When the cutting speed was 110 m/min, the friction coefficients in order from low to high are CT, WT, CWT, and NT. And the friction coefficients in order from low to high are WT, CT, CWT, and NT when the cutting speed is 80 m/min. The characteristics of the CWT to reduce the coefficient of friction are not obvious.
- (4) Compared with the NT, the adhesive height of CT, WT, and CWT was reduced by 28.6%, 37.9%, and 59.4%, respectively. This reflected that the anti-adhesive property of CWT is significantly better than WT and CT. Meanwhile, the wear of CWT in these experiments was normal wear. It means the CWT can effectively protect the hard coating and extend the coating life.
- (5) In general, the effect of combining soft and hard coatings is beyond the superposition of respective effects of soft and hard coatings. Therefore, the CWT improves the cutting performance and is more suitable for dry cutting CFRP materials than other tools.

Funding information This work was supported by the National Natural Science Foundation of China (Grant No. 51505399), the Natural Science Foundation of Fujian Province of China (Grant No. 2017 J05088), and the Jiangsu Key Laboratory of Precision and Micro-Manufacturing Technology.

References

1. Che DM, Saxena I, Han PD, Guo P, Ehmann KF (2014) Machining of carbon fiber reinforced plastics/polymers: a literature review. *J Manuf Sci E-T Asme* 136(3):034001
2. Xing YQ, Deng JX, Zhang GD, Wu Z, Wu FF (2017) Assessment in drilling of C/C-SiC composites using brazed diamond drills. *J Manuf Process* 26:31–43
3. Yang HJ, Chen Y, Xu JH, Ladonne M, Lonfrier J, Fu YC (2019) Tool wear mechanism in low-frequency vibration-assisted drilling of CFRP/Ti stacks and its individual layer. *Int J Adv Manuf Technol* 104:2539–2551
4. Alonso U, Calamaz M, Girot F, Iriondo E (2019) Influence of flutenumber and stepped bit geometry when drilling CFRP/Ti6Al4V stacks. *J Manuf Process* 39:356–370
5. Wang XM, Zhang LC (2003) An experimental investigation into the orthogonal cutting of unidirectional fibre reinforced plastics. *Int J Mach Tool Manu* 43(10):1015–1022
6. Dandekar CR, Shin YC (2012) Modeling of machining of composite materials: a review. *Int J Mach Tool Manu* 57:102–121
7. Jia ZY, Fu R, Niu B, Qian BW, Bai Y, Wang FJ (2016) Novel drillstructure for damage reduction in drilling CFRP composite. *Int J Mach Tool Manu* 110:55–65
8. Wang XC, Shen XT, Yan GD, Sun FH (2017) Evaluation of boron-doped-microcrystalline/nanocrystalline diamond composite coatings in drilling of CFRP. *Surf Coat Tech* 330:149–162
9. Li M, Soo SL, Aspinwall DK, Pearson D, Leahy W (2018) Study on tool wear and workpiece surface integrity following drilling of CFRP laminates with variable feed rate strategy. *Procedia CIRP* 71: 407–412
10. Wang X, Shen X, Zeng C, Sun F (2018) Combined influences of tool shape and as-deposited diamond film on cutting performance of drills for CFRP machining. *Surf Coat Tech* 347:390–397
11. Geier N, Paulo Davim J, Szalay T (2019) Advanced cutting tools and technologies for drilling carbon fibre reinforced polymer (CFRP) composites: a review. *Compos Part A-Appl S* 125:105552
12. Kuo C, Wang C, Ko S (2018) Wear behaviour of CVD diamond-coated tools in the drilling of woven CFRP composites. *Wear* 398-399:1–12
13. Wang X, Kwon PY, Sturtevant C, Kim D, Lantrip J (2013) Tool wear of coated drills in drilling CFRP. *J Manuf Process* 15(1):127–135
14. Karpát Y, Deger B, Bahtiyar O (2014) Experimental evaluation of polycrystalline diamond tool geometries while drilling carbon fiber-reinforced plastics. *Int J Adv Manuf Technol* 71:1295–1307
15. Montoya M, Calamaz M, Gehin D, Girot F (2013) Evaluation of the performance of coated and uncoated carbide tools in drilling thick CFRP/aluminium alloy stacks. *Int J Adv Manuf Technol* 68:2111–2120
16. Hussein R, Sadek A, Elbestawi MA, Attia MH (2019) Elimination of delamination and burr formation using high-frequency vibration-assisted drilling of hybrid CFRP/Ti6Al4V stacked material. *Int J Adv Manuf Technol* 105:859–873

17. Xu J, Li C, Chen M, Mansori MEI, Ren F (2019) An investigation of drilling high-strength CFRP composites using specialized drills. *Int J Adv Manuf Technol* 103:3425–3442
18. Gaugel S, Sripathy P, Haeger A, Meinhard D, Bernthaler T, Lissek F, Kaufeld M, Knoblauch V, Schneider G (2016) A comparative study on tool wear and laminate damage in drilling of carbon-fiber reinforced polymers (CFRP). *Compos Struct* 155:173–183
19. Liang XL, Liu ZQ, Liu WT, Li XJ (2019) Sustainability assessment of dry turning Ti-6Al-4V employing uncoated cemented carbide tools as clean manufacturing process. *J Clean Prod* 214:279–289
20. Abdalla HS, Baines W, McIntyre G, Slade C (2007) Development of novel sustainable neat-oil metal working fluids for stainless steel and titanium alloy machining. Part 1. Formulation development. *Int J Adv Manuf Technol* 34:21–33
21. Lian YS, Mu CL, Wang L, Yao B, Deng JX, Lei ST (2018) Numerical simulation and experimental investigation on friction and wear behaviour of micro-textured cemented carbide in dry sliding against TC4 titanium alloy balls. *Int J Refract Met H* 73: 121–131
22. Klocke F, Eisenblatter G (1997) Dry cutting. *CIRP Ann* 46(2):519–526
23. Lawal SA, Choudhury IA, Nukman Y (2012) Application of vegetable oil-based metalworking fluids in machining ferrous metals—a review. *Int J Mach Tool Manu* 52(1):1–12
24. Ma JF, Duong NH, Lei ST (2015) Numerical investigation of the performance of microbump textured cutting tool in dry machining of AISI 1045 steel. *J Manuf Process* 19:194–204
25. Duan R, Deng JX, Lei ST, Ge DL, Liu YY, Li XM (2019) Effect of derivative cutting on machining performance of micro textured tools. *J Manuf Process* 45:544–556
26. Yuan W, Tang Y, Yang XJ, Liu B, Wan ZP (2013) On the processing and morphological aspects of metal fibers based on low-speed multi-tooth dry cutting. *Int J Adv Manuf Technol* 66(5–8):1147–1157
27. Lian YS, Deng JX, Li SP, Xing YQ, Chen YY (2013) Preparation and cutting performance of WS₂ soft-coated tools. *Int J Adv Manuf Technol* 67(5–8):1027–1033
28. Caprino G, Delorio I, Nele L, Santo L (1996) Effect of tool wear on cutting forces in the orthogonal cutting of unidirectional glass fibre-reinforced plastics. *Compos Part A Appl S* 27(5):409–415
29. Grilo TJ, Paulo RMF, Silva CRM, Davim JP (2013) Experimental delamination analyses of CFRPs using different drill geometries. *Compos Part B Eng* 45(1):1344–1350
30. Kwon B, Mai NDD, Cheon ES, Ko SL (2020) Development of a step drill for minimization of delamination and uncut in drilling carbon fiber reinforced plastics (CFRP). *Int J Adv Manuf Technol* 106:1291–1301

Publisher's note Springer Nature remains neutral with regard to jurisdictional claims in published maps and institutional affiliations.